QoS-Driven MAC-Layer Resource Allocation for Wireless Mesh Networks with Non-Altruistic Node Cooperation and Service Differentiation

Ho Ting Cheng, *Student Member, IEEE*, and Weihua Zhuang, *Fellow, IEEE*

***Abstract*— Node cooperation has been demonstrated promising in system performance improvement for wireless networks. To effectively provision packet-level quality-of-service (QoS) in wireless mesh networks (WMNs) supporting heterogeneous traffic, medium access control (MAC) with service differentiation is imperative. In this paper, we study the problem of non-altruistic non-reciprocal node cooperative resource allocation for WMNs with QoS support, taking subcarrier allocation, power allocation, partner selection/allocation, service differentiation, and packet scheduling into account. Due to the NP hardness of our resource allocation problem, we propose two low-complexity yet effective approaches based on the Karush-Kuhn-Tucker (KKT) interpretations, tailored for WMNs with QoS assurance and MAC-layer service differentiation. Further, simulation results show that both proposed approaches can effectively provision packet-level QoS and enhance system performance. Our study also sheds some light on the question of whether and when non-altruistic node cooperation is beneficial to WMNs.**

***Index Terms*—Karush-Kuhn-Tucker (KKT), non-altruistic node cooperation, quality-of-service (QoS) provisioning, resource allocation, service differentiation, wireless mesh network (WMN).**

I. Introduction

WIRELESS mesh networking has emerged as a promising solution for future broadband wireless access [2]. Wireless mesh networks (WMNs) generally comprise gateways, mesh routers, and mesh clients, organized in a three-tier hierarchical architecture [2]. Recently, wireless mesh networking for suburban/rural residential areas has been attracting a lot of attentions (e.g., Wray WMNs [3]). Mesh routers can be set up at premises in a neighborhood, forming a resilient mesh backbone and providing an all-wireless environment [3].

As increasing throughput in a WMN is the key to the success of providing an all-wireless environment, different resource allocation strategies have been proposed to provide a high-speed mesh backbone with quality-of-service (QoS) assurance (e.g., [4]). To further enhance the system performance, *cooperative diversity* or node cooperation can be employed to achieve a spatial diversity gain by way of a virtual antenna array formed by multiple wireless nodes in a distributed fashion [5]. In fact, node cooperation has been demonstrated promising in improving the spectral and power efficiency of wireless networks without additional complexity of multiple antennas [6]. The basic idea behind node cooperation rests on the observation that the signal transmitted by a source node can be overheard by other nodes in a wireless environment. The source and its *partner(s)* can jointly process and transmit their information, thereby creating a virtual antenna array and achieving a desired diversity-multiplexing tradeoff [7]. Compared to traditional co-located multi-antenna techniques, node cooperation can provide a comparable spatial diversity gain without imposing extra hardware complexity.

Although there exists a rich body of research work on node cooperation in the literature [6]–[17], packet-level scheduling is mostly neglected, and the issue of QoS support and provisioning has not been carefully addressed. This phenomenon stems from the fact that previous research work mainly focuses on issues related to the physical layer. In this work, our goal is to devise an efficient and effective node cooperative resource allocation strategy tailored for WMNs with heterogenous traffic. In particular, we focus on medium access control (MAC)-layer resource allocation in WMNs with QoS assurance and service differentiation. We consider regenerative mesh nodes and non-altruistic node cooperation, meaning that there is no pure relay in the system. Further, the node cooperation of interest is non-reciprocal, meaning that one node assists its neighbor but does not necessarily receive help from that neighbor. We also consider prioritized node cooperation so as to realize the notion of service differentiation.

The main contributions and significance of our work are two-fold:

1) We study the problem of non-altruistic node cooperative resource allocation for WMNs with QoS support, taking subcarrier allocation, power allocation, partner selection/allocation, service differentiation, and packet scheduling into account. Thanks to the Karush-Kuhn-Tucker (KKT) interpretations, we propose two resource allocation approaches tailored for the WMN of interest. Both approaches are shown to be effective in providing QoS assurance and service differentiation. Further, our approaches are of low complexity, leading to viable candidates for practical implementation;
2) Simulation results show that both proposed approaches are effective in packet-level QoS provisioning and system

Manuscript received May 7, 2009; revised September 18, 2009; accepted October 15, 2009. The associate editor coordinating the review of this paper and approving it for publication was J. M. Shea.

This research was supported by research grants from the Natural Science and Engineering Research Council (NSERC) of Canada. This research is presented in part in a paper accepted for presentation in IEEE Globecom 2009 [1].

The authors are with the Centre for Wireless Communications, Department of Electrical and Computer Engineering, University of Waterloo, 200 University Avenue West, Waterloo, Ontario, Canada N2L 3G1 (e-mail: {htcheng, wzhuang}@bbcr.uwaterloo.ca).

Digital Object Identifier 10.1109/TWC.2009.090502

performance enhancement over their counterparts. Our results demonstrate that the proposed approaches are less vulnerable to the changes in the system parameters such as the accuracy of traffic load estimates. Further, our study reveals a critical principle that whether node cooperation is beneficial depends upon the nature of node cooperation, the mode of network operation, and the traffic pattern.

The remainder of this paper is organized as follows. Related work is given in Section II. The system model is described in Section III. The problem of non-altruistic node cooperative resource allocation for WMNs with QoS support is described in Section IV. Two proposed QoS-driven resource allocation approaches with node cooperation are presented in Section V. Performance evaluation is given in Section VI. Finally, conclusions are presented in Section VII.

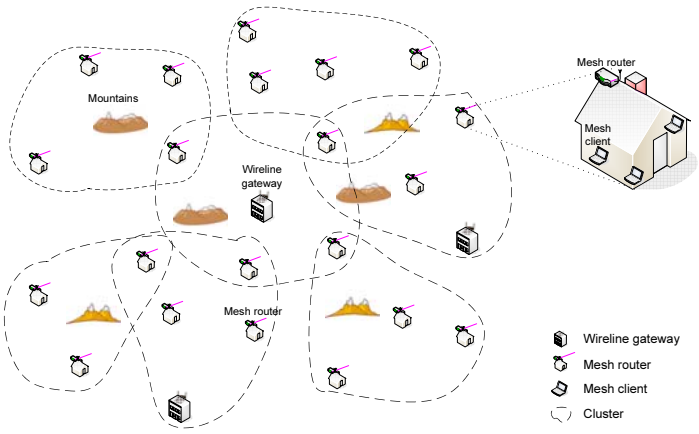

Fig. 1. An illustration of a typical WMN for suburban/rural residential areas.

II. Related Work

In the literature, there exists a rich body of research work on node cooperation [6]–[17]. Besides information-theoretic studies [7], most recent work on the topic of node cooperation can be classified into two groups: 1) distributed space-time coding design; and 2) resource allocation with relay selection. The first group focuses on the design and performance evaluation of distributed space-time coding (e.g., [6,8]). Spectral efficiency can be further improved by means of dirty paper coding applied at the transmitters [9]. With appropriate detection techniques, an additional diversity order can be attained in time-varying wireless channels [10]. However, most node cooperation strategies based on distributed space-time coding conceive the existence of pure relay nodes, which is not always feasible in practical WMNs. The second group aims at relay selection and resource allocation. Partner matching algorithms based on graph theory are proposed in [11], the objective of which is to optimize the energy efficiency; however, energy consumption is not a concern in WMNs. In [12], a distributed cooperative MAC protocol for multi-hop networks is proposed for relay selection. Game theory and auction theory are also employed to derive node cooperation strategies and cooperative resource allocation solutions (e.g., [13,14]). The performance results of the aforementioned approaches can be appealing; however, powerful central controllers are mostly required to execute those algorithms. In the case of austere suburban and rural environments, distributed control is preferred, yet directly applying those approaches to WMNs with decentralized control can be ineffective or inefficient. On the other hand, many of the existing partner selection schemes consider only measured (instantaneous) signal-to-noise ratios in choosing a partner (e.g., [7]), and most of the existing approaches focus on altruistic node cooperation. In the context of non-altruistic node cooperation, the availability of a potential partner and its QoS requirement should also be taken into account. In [15,16], the problem of partner selection for non-altruistic node cooperation is studied. Three partner selection schemes with power control are proposed in [15] for balancing transmit power and system performance, whereas two partner selection schemes are proposed in [16] so as to minimize the average outage probability. However, MAC-layer service differentiation is not addressed, for only a single class of traffic is considered in the aforementioned work. In [17], Zhang *et al.* propose a simple two-step scheme for the system throughput maximization problem with physical-layer QoS assurance. Without considering beneficial node cooperation, however, system performance can be undermined. In addition, both packet scheduling and packet-level QoS support are not taken into consideration, plausibly elevating the packet dropping rates for real-time traffic.

In this work, we propose two low-complexity QoS-driven node cooperative resource allocation approaches tailored for WMNs with heterogeneous traffic. Our proposed approaches are demonstrated efficient yet effective in providing packet-level QoS assurance and facilitating MAC-layer service differentiation.

III. System Model

A. Network Model

We consider an orthogonal frequency division multiplexing (OFDM)-based WMN for suburban or rural residential areas, consisting of wireline gateways attached to the Internet backbone and a number of mesh routers and mesh clients scattered around, rendering a hierarchical multi-hop network (see Fig. 1). In specific, mesh routers mounted on the rooftops of the premises comprise a wireless mesh backbone, while mesh clients (e.g., laptops) associated with their closest mesh router constitute various access networks. The system model takes account the austere suburban and rural networking environments, which thwarts one-hop direct communications as opposed to multi-hop transmissions, providing ease of deployment and offering greater coverage of wireless access [2]. Mesh routers are assumed stationary and hence the channel gains can be estimated accurately. We consider that traffic traverses from mesh clients to mesh routers to the gateway only. Each mesh node is equipped with one transceiver having an omni-directional antenna, so that it cannot transmit and receive at the same time. To provide network stability and increase throughput, we assume that there is an efficient node clustering algorithm in place for the wireless mesh backbone [4], so that the notion of frequency reuse is taken into consideration, the cochannel interference level is bounded,

and each cluster is assigned a set of subcarriers. Consider a synchronized WMN, in which time is partitioned into frames, each containing a number of DATA slots. Two classes of traffic are considered, namely 1) rate-guaranteed (RG) traffic and 2) best-effort (BE) traffic. In particular, the RG traffic has a minimum data rate requirement and a delay bound requirement, whereas the BE traffic has no QoS requirement. Call admission control (CAC) is assumed in place such that the QoS requirements of an admitted RG traffic flow can be met. Node cooperation is considered and triggered as long as it is feasible and beneficial for system performance. In fact, there are many plausible node cooperation scenarios in the WMN of interest; however, in this work, we focus on a node cooperation scenario where clustermembers cooperatively transmit their packets to a clusterhead.

B. Node Cooperation

Consider a transmission scenario involving three wireless nodes, namely Node *S*, Node *R*, and Node *D*. Node *S* is to transmit data to Node *D*, while Node *R* is viewed as a relay to help Node *S* forward the data to Node *D*. We employ the Cooperation Protocol I suggested in [5] as our node cooperation strategy throughout this paper, and consider the decode-and-forward (DF) mode of cooperation (i.e., regenerative mesh nodes). In the first timeslot, Node *S* transmits a packet to both Node *R* and Node *D*. In the second timeslot, Node *R* forwards the packet received from Node *S* to Node *D*, while Node *S* transmits another packet to Node *D*. Notice that, in this cooperation protocol, Node *D* receives two copies of the first packet and one copy of the second packet in two timeslots. In traditional cooperative networks with nodes employing full transmit power, the achievable throughput per timeslot due to cooperative transmissions can be higher than direct transmissions, thanks to both spatial multiplexing gain and power gain. Unlike symbol-level cooperation where continuous symbol transmissions can be feasible, continuous packet transmissions are less realistic. Thus, in this work, we consider that a potential packet-level cooperation opportunity arises in every two timeslots. Following the analysis in [7] for a frequency-flat Rayleigh fading environment, the channel capacity C_{DF} achieved by the DF mode with perfect decoding is given by $C_{DF} = \frac{1}{2}\log_2\left((1+\gamma_{SD})^2+\gamma_{RD}\right)$, where $\gamma_{XY} = E_{XY}|h_{XY}|^2/\sigma^2$ with $E_{XY}(\geq 0)$ being the received average energy at Node Y from Node X, $X, Y \in \{S, R, D\}$, h_{XY} the Rayleigh fading coefficient for the $X \rightarrow Y$ link modeled as an independent zero-mean complex Gaussian random variable with unit variance, and σ^2 the noise-plus-cochannel interference power level. In the case of non-altruistic node cooperation, due to the necessity of splitting the transmit power, C_{DF} is given by $C_{DF} = \frac{1}{2}\log_2\left((1+a_S\gamma_{SD})^2+a_R\gamma_{RD}\right)$, where a_X is the scaling factor for the transmit power of Node X, i.e., $0 \leq a_X \leq 1$. Following the analysis given in [7], it can be proved that arbitrarily positive power allocation has no impact on the diversity performance in the DF cooperation mode with perfect decoding. By the same token, it can be further proved that, with m potential relays, choosing the single best relay is sufficient to achieve the full diversity order in the DF cooperation mode with perfect decoding and arbitrarily positive power allocation. It is noteworthy that the case of $a_S = 1$ corresponds to the scenario of *altruistic* node cooperation. Compared to the channel capacity achieved by ordinary direct transmissions, denoted by $C_d = \log_2(1+\gamma_{SD})$, we can envision that a non-altruistic cooperative transmission may not always be advantageous over an ordinary direct transmission. Therefore, for the sake of overall system performance, node cooperation among mesh nodes should be considered in a holistic manner, to be discussed in Section V.

IV. QoS-Driven Non-Altruistic Node Cooperative Resource Allocation

There are various system constraints associated with the non-altruistic node cooperative resource allocation problem for WMNs. Let M, N, and L denote the number of mesh nodes, the number of subcarriers available, and the number of timeslots (i.e., DATA slots) in a frame, respectively. The sum of the (non-negative) transmit power of each mesh node on the (allocated) subcarriers is bounded by a maximum power level:

$$\sum_{n=1}^{N} p_{m,n}^{l} \leq P_m^{\max}, \forall m, l \quad \text{and} \quad p_{m,n}^{l} \geq 0, \forall m, n, l \qquad (1)$$

where $p_{m,n}^{l}$ is the transmit power of the m^{th} node over the n^{th} subcarrier on the l^{th} timeslot and $P_m^{\max}$ is the maximum power constraint of the m^{th} node. With the help of node clustering, a number of subcarriers are allocated to each cluster. Here, we consider the case where each subcarrier can only be allocated to one transmission link without cooperation or at most two transmission links with node cooperation (i.e., a direct link and an assisted link) in a cluster. If node cooperation is employed, both a source node and its partner transmit data over the same subcarrier(s). In addition, since choosing the best partner is sufficient in terms of diversity performance [7], a node can have at most one partner at a time on condition that the node cooperation is favorable. The aforementioned constraints can be formulated as follows:

$$\sum_{m=1}^{M} c_{m,n}^{l} \leq 1 + \sum_{u=1,u\neq m}^{M} z_{mu}, \forall n, l \quad \text{and} \quad c_{u,n}^{l} = c_{m,n}^{l}, \quad \text{when } z_{mu} = 1, \forall m, u, n, l \qquad (2)$$

$$\sum_{m=1,m\neq u}^{M} z_{mu} \leq 1, \forall u \quad \text{and} \quad \sum_{u=1,u\neq m}^{M} z_{mu} \leq 1, \forall m \qquad (3)$$

$$c_{m,n}^{l} \in \{0,1\}, \forall m, n, l \quad \text{and} \quad z_{mu} \in \{0,1\}, \forall m, u \qquad (4)$$

where $c_{m,n}^{l}$ is an indicator of allocating the n^{th} subcarrier to the m^{th} node on the l^{th} timeslot and z_{mu} is the indicator of node cooperation offered to the m^{th} node by the u^{th} node. Notice that, in general, $z_{yx} \neq z_{xy}, \forall x, y$, as the node cooperation considered in this work is non-reciprocal (i.e., asymmetric). For the sake of notational convenience, we set $z_{mm} = 1, \forall m$. Provided that node cooperation is in place, the transmit power of a node is split into two segments, one dedicated to its direct transmissions and the other to the

assisted transmissions for its partner:

$$\sum_{m=1}^{M} z_{mu}a_{mu} = 1, \forall u \quad \text{and} \quad 0 \le a_{mu} \le 1, \forall m, u \tag{5}$$

with a_{mu} being the normalized portion of the total transmit power of the u^{th} node for assisting the m^{th} node's transmissions. Let $\mathcal{M}_1$ and $\mathcal{M}_2$ be the set of RG nodes and that of BE nodes, respectively, i.e., $M = |\mathcal{M}_1| + |\mathcal{M}_2|$. In our problem formulation, we take the minimum rate requirements of the RG nodes in the current frame, if any, into account:

$$R_m(\mathbf{c}, \mathbf{p}, \mathbf{a}, \mathbf{z}) \ge R_m^d, \forall m \tag{6}$$

where R_m^d is the (instantaneous) transmission rate demand of the m^{th} node in the current frame (i.e., $R_m^d > 0, \forall m \in \mathcal{M}_1$ and $R_m^d = 0, \forall m \in \mathcal{M}_2$) and $R_m(\mathbf{c}, \mathbf{p}, \mathbf{a}, \mathbf{z})$ is the achievable data rate of the m^{th} node, which can be computed by [6]

$$R_m(\mathbf{c}, \mathbf{p}, \mathbf{a}, \mathbf{z}) = \sum_{n=1}^{N}\sum_{l=1}^{L} \frac{1}{2} c_{m,n}^l \log_2 \left(\left(1 + a_{mm} g_{mm,n}^l p_{m,n}^l\right)^2 + \sum_{u=1, u\neq m}^{M} z_{mu} a_{mu} g_{mu,n}^l p_{u,n}^l \right). \tag{7}$$

In (7), $\mathbf{c} = \left[c_{m,n}^l\right]_{M\times N\times L}$, $\mathbf{p} = \left[p_{m,n}^l\right]_{M\times N\times L}$, $\mathbf{a} = [a_{mu}]_{M\times M}$, $\mathbf{z} = [z_{mu}]_{M\times M}$, and $g_{mu,n}^l = \varphi G_{mu,n}^l/\sigma_n^2$, where φ is a bit-error-rate (BER) measure, $G_{mu,n}^l$ the channel gain from the u^{th} node to the receiver of the m^{th} node's transmissions over the n^{th} subcarrier on the l^{th} timeslot, and σ_n^2 the aggregate noise-plus-cochannel interference power on the n^{th} subcarrier. Notice that constraint (2) is implicitly incorporated in (7). With the aforesaid system constraints, different objective functions can be considered. Here, we employ the well-known utility maximization framework to abstract our objective function. Let $U_m(R_m(\mathbf{c}, \mathbf{p}, \mathbf{a}, \mathbf{z})|\mathbf{\Theta})$ denote the utility function of the m^{th} node and $\mathbf{\Theta} \in \{1, 2\}$ the utility selector. The objective function is given by

$$\sum_{m=1}^{M} U_m(R_m(\mathbf{c}, \mathbf{p}, \mathbf{a}, \mathbf{z}))|\mathbf{\Theta}) = \begin{cases} \sum_{m=1}^{M} R_m(\mathbf{c}, \mathbf{p}, \mathbf{a}, \mathbf{z}), & \text{when } \mathbf{\Theta} = 1 \\ \sum_{m=1}^{M} -\left[-\ln\left(\frac{R_m(\mathbf{c},\mathbf{p},\mathbf{a},\mathbf{z})}{A}\right)\right]^{\kappa}, & \text{when } \mathbf{\Theta} = 2 \end{cases} \tag{8}$$

where A is a sufficiently large constant such that $0 < R_m/A < 1, \forall m$ [18]. Thus, the objective function is to maximize the system throughput when $\mathbf{\Theta} = 1$, to achieve proportional fairness when $\mathbf{\Theta} = 2$ and $\kappa = 1$, and to achieve max-min fairness when $\mathbf{\Theta} = 2$ and $\kappa \to \infty$, respectively. In practice, the choice of $\mathbf{\Theta}$ is contingent on the purpose of the networking application and/or the prerogative of a system designer. Other system performance can also be optimized by means of utility functions (e.g., a tradeoff between throughput and fairness [19]). In light of the fact that traffic demands and interference levels vary over time, we need to update our resource allocation solution from time to time. Therefore, we consider that the node cooperation between a source node and its partner is committed merely for an active resource allocation interval.

Problem Formulation: Consider the following non-altruistic node cooperative resource allocation optimization problem (NCRAOP)

$$\max_{\mathbf{c},\mathbf{p},\mathbf{a},\mathbf{z}} \left\{ \sum_{m=1}^{M} U_m\left(R_m(\mathbf{c}, \mathbf{p}, \mathbf{a}, \mathbf{z})|\mathbf{\Theta}\right) \right\} \tag{9}$$

$$\text{subject to} \quad (1), (3), (4), (5), (6), \quad \text{and} \quad \sum_{m=1}^{M} c_{m,n}^l \le 1, \forall n, l$$

where $\mathbf{c}, \mathbf{p}, \mathbf{a}$, and $\mathbf{z}$ are the *optimization variables*. By reducing the well-known NP-complete *number partitioning problem* to the NCRAOP, it can be proved that the NCRAOP is an NP-hard problem. A summary of important symbols used in this paper is given in Table I for easy reference.

V. Proposed Resource Allocation Approaches with Node Cooperation

A. KKT Interpretations

In general, solving the NP-hard NCRAOP requires exponential time complexity [20]. To design an efficient and effective resource allocation approach to solve the NCRAOP, we consider the Lagrangian of the NCRAOP and the KKT conditions. Due to space limitations, we only present some key results here.

1) Subcarrier Allocation Criterion: For the n^{th} subcarrier and the l^{th} timeslot, choose

$$m^* = \arg\max_m \left\{ \left(U_m'\left(R_m(\mathbf{c}, \mathbf{p}, \mathbf{a}, \mathbf{z})|\mathbf{\Theta}\right) + {\xi^{(1)}}_m\right) \cdot \frac{\partial R_m(\mathbf{c}, \mathbf{p}, \mathbf{a}, \mathbf{z})}{\partial c_{m,n}^l} \right\} \tag{10}$$

where ${\xi^{(1)}}_m$ is the Lagrange multiplier for constraint (6), and set $c_{m^*,n}^l = 1$.

2) Partner Allocation Criterion: For the u^{th} node, choose m^* such that

$$m^* = \arg\max_{m\neq u} \left\{ \frac{U_m'\left(R_m(\mathbf{c}, \mathbf{p}, \mathbf{a}, \mathbf{z})|\mathbf{\Theta}\right)}{a_{mu}} \frac{\partial R_m(\mathbf{c}, \mathbf{p}, \mathbf{a}, \mathbf{z})}{\partial z_{mu}} \right\} \tag{11}$$

and set $z_{m^*u} = 1$.

3) Partner Selection Criterion: For the m^{th} node, choose u^* such that

$$u^* = \arg\max_{u\neq m} \left\{ \frac{U_m'\left(R_m(\mathbf{c}, \mathbf{p}, \mathbf{a}, \mathbf{z})|\mathbf{\Theta}\right)}{a_{mu}} \frac{\partial R_m(\mathbf{c}, \mathbf{p}, \mathbf{a}, \mathbf{z})}{\partial z_{mu}} \right\} \tag{12}$$

and set $z_{mu^*} = 1$.

Notice that, in general, the results obtained from the partner selection criterion and that from the partner allocation criterion are not the same. The partner selection criterion refers to choosing the best relay for a particular source node, whereas the partner allocation criterion refers to allocating a relay node to the best source node. In a nutshell, the partner selection criterion is to maximize the node-wise utility, while the partner allocation criterion is to maximize the network-wise utility.

TABLE I
SUMMARY OF IMPORTANT SYMBOLS.

Symbol	Definition
M	number of mesh nodes in the WMN
N	number of available subcarriers in the WMN
L	number of timeslots (i.e., DATA slots) in a frame
$p_{m,n}^{l}$	transmit power of the m^{th} node over the n^{th} subcarrier on the l^{th} timeslot
$P_{m}^{\max}$	maximum power constraint of the m^{th} node
$c_{m,n}^{l}$	indicator of allocating the n^{th} subcarrier to the m^{th} node on the l^{th} timeslot
z_{mu}	indicator of node cooperation offered to the m^{th} node by the u^{th} node
a_{mu}	normalized portion of the total transmit power of the u^{th} node for assisting the m^{th} node
$R_m(\cdot)$	achievable data rate of the m^{th} node
R_m^d	(instantaneous) transmission rate demand of the m^{th} node
$U_m(\cdot)$	utility function of the m^{th} node
Θ	utility selector
ρ	tunable system parameter to balance cooperation and non-cooperation
$\mathcal{N}_m^l$	set of subcarriers allocated to the m^{th} node on the l^{th} timeslot
T	polling time interval
λ	Poisson arrival rate for BE traffic

B. Examples

To better understand the conceptual implications of our subcarrier allocation criterion and partner selection/allocation criterion, we consider the following three objective functions, namely 1) system throughput maximization, 2) proportional fairness, and 3) max-min fairness. For presentation clarity, we assume ${\xi^{(1)}}_m = 0$.

1) System Throughput Maximization ($\mathbf{\Theta} = 1$): $U_m\left(R_m\left(\cdot\right)|\mathbf{\Theta}\right) = R_m\left(\cdot\right)$ and hence $U_m'\left(R_m\left(\cdot\right)|\mathbf{\Theta}\right) = 1$; therefore, the subcarrier allocation criterion given in (10) and the partner selection criterion given in (12) become

$$m^* = \arg\max_{m} \left\{ \log_2 \left(\left(1 + a_{mm} g_{mm,n}^{l} p_{m,n}^{l}\right)^2 + \sum_{u=1, u\neq m}^{M} z_{mu} a_{mu} g_{mu,n}^{l} p_{u,n}^{l} \right) \right\} \tag{13}$$

and

$$u^* = \arg\max_{u\neq m} \left\{ \sum_{n=1}^{N} \sum_{l=1}^{L} c_{m,n}^{l} g_{mu,n}^{l} p_{u,n}^{l} \cdot \frac{1}{\left(1 + a_{mm} g_{mm,n}^{l} p_{m,n}^{l}\right)^2 + \sum_{u\neq m} z_{mu} a_{mu} g_{mu,n}^{l} p_{u,n}^{l}} \right\} \tag{14}$$

respectively. Thus, given the power allocation (i.e., $\mathbf{a}, \mathbf{p}$) and partner selection (i.e., $\mathbf{z}$), the condition (13) implies that the larger throughput the m^{th} node can contribute over the n^{th} subcarrier on the l^{th} timeslot, the better the n^{th} subcarrier on the l^{th} timeslot is assigned to the m^{th} node (i.e., $c_{m,n}^{l} = 1, \exists_{m,n,l}$). Likewise, given the power allocation and subcarrier allocation, the condition (14) indicates that we should choose a partner who can contribute the largest marginal increase in the achievable data rate. Therefore, both criteria agree with the notion of throughput maximization. Notice that in the case of non-cooperation (i.e., $z_{mu} = 0$), the condition (13) reduces to the well-known subcarrier allocation criterion for throughput maximization [21].

2) Proportional Fairness ($\mathbf{\Theta} = 2$ and $\kappa = 1$): $U_m\left(R_m\left(\cdot\right)|\mathbf{\Theta}\right) = \ln\left(\frac{R_m(\cdot)}{A}\right)$ and hence $U_m'\left(R_m\left(\cdot\right)|\mathbf{\Theta}\right) = 1/R_m\left(\cdot\right)$; therefore, the conditions (10) and (12) become

$$m^* = \arg\max_{m} \left\{ \frac{1}{R_m\left(\cdot\right)} \log_2 \left(\left(1 + a_{mm} g_{mm,n}^{l} p_{m,n}^{l}\right)^2 + \sum_{u=1, u\neq m}^{M} z_{mu} a_{mu} g_{mu,n}^{l} p_{u,n}^{l} \right) \right\} \tag{15}$$

and

$$u^* = \arg\max_{u\neq m} \left\{ \frac{1}{R_m\left(\cdot\right)} \sum_{n=1}^{N} \sum_{l=1}^{L} c_{m,n}^{l} g_{mu,n}^{l} p_{u,n}^{l} \cdot \frac{1}{\left(1 + a_{mm} g_{mm,n}^{l} p_{m,n}^{l}\right)^2 + \sum_{u\neq m} z_{mu} a_{mu} g_{mu,n}^{l} p_{u,n}^{l}} \right\} \tag{16}$$

respectively. As seen, it is more likely for a mesh node to get an extra subcarrier and/or a partner if its data rate obtained is small, whereas it is less likely to assign an extra subcarrier or a partner to a node whose data rate obtained is already very high. Thus, both criteria match with the notion of proportional fairness.

3) Max-min Fairness ($\mathbf{\Theta} = 2$ and $\kappa \to \infty$): $U_m\left(R_m\left(\cdot\right)|\mathbf{\Theta}\right) = -\left[-\ln\left(\frac{R_m(\mathbf{c},\mathbf{p},\mathbf{a},\mathbf{z})}{A}\right)\right]^{\kappa}$, and hence $U_m'\left(R_m\left(\cdot\right)|\mathbf{\Theta}\right) = \kappa\left[-\ln\left(R_m(\cdot)/A\right)\right]^{\kappa-1}/R_m(\cdot)$. Since $0 < R_m(\cdot)/A < 1$, $\left[-\ln\left(R_m(\cdot)/A\right)\right]^{\kappa-1}$ becomes a dominant term as $\kappa \to \infty$. Hence, the conditions (10) and (12) become

$$m^* = \arg\min_{m} R_m(\cdot) \quad \text{and} \quad u^* = \arg\min_{u\neq m} R_m(\cdot) \tag{17}$$

respectively. Thus, we tend to assign subcarriers and partners to the nodes which have minimal achievable data rates, realizing the notion of max-min fairness.

In the following subsections, we propose a centralized resource allocation approach and a distributed resource allocation approach to solve the NCRAOP in Section V-C and Section V-D, respectively.

C. Proposed Approach with Centralized Control

In order to obtain the global optimal solutions to the NCRAOP, subcarrier allocation, partner selection/allocation, and power allocation should be jointly considered, which brings about very high computational cost. To devise an efficient yet effective node cooperative resource allocation strategy with centralized control, we propose a four-phase resource allocation approach with QoS assurance and service differentiation. Specifically, in Phase 1, we fix the power allocation and then solve the NCRAOP without considering node cooperation; In Phase 2, we perform water filling for power allocation to improve the system performance; In Phase 3, we allow node cooperation, if feasible and favorable, so as to add an additional performance gain to the system; In Phase 4, we perform water filling for power allocation again providing the solutions of subcarrier allocation and partner allocation, thereby further improving the system performance.

Consider a simple MAC protocol to illustrate the notion of packet scheduling for our proposed approach. Time is partitioned into frames, each of which is further divided into a beacon slot, a control slot, and L DATA slots. Each RG node estimates the traffic load (i.e., both the local traffic load and the relay traffic load) by averaging the rate requirement over a fixed estimation window (e.g., 100ms) on a regular basis. In the control slot, a clusterhead collects the traffic demand from its clustermembers at the beginning of each active resource allocation interval (i.e., by polling periodically). Then, the clusterhead executes the proposed centralized resource allocation and announces a resource allocation decision in the next beacon slot. In the DATA slots, nodes transmit their information according to the resource allocation decision.

Phase-1: With uniform power allocation and no node cooperation (i.e., $z_{mu} = 0$ and $a_{mu} = 0, \forall m \neq u$), the NCRAOP can be reduced to the following resource allocation optimization problem

$$\max_{\mathbf{c}} \left\{ \sum_{m=1}^{M} U_m \left(R_m \left(\mathbf{c} \right) | \mathbf{\Theta} \right) \right\} \tag{18}$$

$$\text{subject to } (6), \ \sum_{m=1}^{M} c_{m,n}^{l} \leq 1, \forall n, l, \quad \text{and } \ c_{m,n}^{l} \in \{0,1\}, \forall m, n, l \tag{19}$$

and the subcarrier allocation criterion given in (10) is as follows. For the n^{th} subcarrier and the l^{th} timeslot, choose m^* such that $m^* = \arg\max_m \left\{ \left(U_m' \left(R_m \left(\mathbf{c} \right) | \mathbf{\Theta} \right) + {\xi^{(1)}}_m \right) \log_2 \left(1 + g_{mm,n}^{l} p_{m,n}^{l} \right) \right\}$. The variable ${\xi^{(1)}}_m$ is updated iteratively by ${\xi^{(1)}}_m = \max \left\{ 0, {\xi^{(1)}}_m - s_m^{(k)} d_m \right\}$, with $s_m^{(k)}$ being the step size at the k^{th} iteration for the m^{th} node and $d_m = R_m(\mathbf{c}) - R_m^d$. With CAC in place, the approach terminates when all the subcarriers are allocated and all the rate requirements are met (i.e., ${\xi^{(1)}}_m = 0, \forall m$), and the subcarrier allocation solution $\mathbf{c}^*$ is obtained such that $\sum_{m=1}^{M} {c^*}_{m,n}^{l} = 1, \forall n, l$.

Phase-2: Perform water filling for optimal power allocation on the allocated subcarriers for each mesh node. Let $R_m(\hat{\mathbf{p}})$ and $R_m(\mathbf{p}^*)$ be the achievable data rate obtained of the m^{th} node with uniform power allocation (i.e., $\hat{\mathbf{p}}$) and that with optimal power allocation (i.e., $\mathbf{p}^*$), respectively. Since $R_m(\mathbf{p}^*) \geq R_m(\hat{\mathbf{p}})$ [22], the QoS demands of the mesh nodes can still be met after transmit power is allocated according to water filling. In a nutshell, Phase-2 resource allocation further improves the Phase-1 resource allocation solutions by employing optimal power allocation, conducing to improved system performance.

Phase-3: Here, we investigate the performance gain due to feasible and favorable node cooperation. Notice that partner *allocation* is feasible in our centralized approach, for a clusterhead can have complete knowledge on which mesh nodes can be the potential partners for a particular mesh node. With the subcarrier allocation solution obtained in Phase 1 and the power allocation solution obtained in Phase 2, the NCRAOP becomes

$$\max_{\mathbf{a},\mathbf{z}} \left\{ \sum_{m=1}^{M} U_m \left(R_m \left(\mathbf{a}, \mathbf{z} \right) | \mathbf{\Theta} \right) \right\} \tag{20}$$

$$\text{subject to } \ (3), (5), (6), \ \text{ and } \ z_{mu} \in \{0,1\}, \forall m, u. \tag{21}$$

Denote ρ (≥ 0) as a tunable system parameter to balance node cooperation and node non-cooperation, i.e., $a_{mu} = \rho a_{uu}, \exists m \neq u$. In fact, ρ indicates the *willingness* of a node to assist another mesh node's transmissions, i.e., the smaller the value of ρ, the less eager is a node to assist the m^{th} node for some m. For some u, if $\sum_{m \neq u} z_{mu} = 1$, then $a_{mu} = \rho a_{uu} (> 0), \exists m \neq u$; otherwise, $a_{uu} = 1$ and $a_{mu} = 0, \forall m \neq u$. On the other hand, in the case of non-altruistic node cooperation, it is conceivable that the value of ρ should be upper bounded (e.g., $\rho \leq 0.5$), as all the mesh nodes have their own data to transmit. Suppose the u^{th} node is to assist the m^{th} node, i.e., $z_{mu} = 1$. Then, the transmit power of the u^{th} node left for cooperation, denoted by P_u^{left}, is given by $P_u^{\text{left}} = P_u^{\max} - a_{uu} \sum_{n=1}^{N} p_{u,n}^{l}$, where $p_{u,n}^{l}$ is obtained from Phase-2. Let $\mathcal{N}_m^l$ be the set of subcarriers allocated to the m^{th} node on the l^{th} timeslot. If the transmit power of the u^{th} node dedicated to node cooperation is uniformly distributed over the subcarriers allocated to the m^{th} node on the l^{th} timeslot, then $\hat{p}_{u,n}^{l} = P_u^{\max} / \sum_{n \in \mathcal{N}_m^l} c_{m,n}^{l}$. Thus, the portion of the transmit power of the u^{th} node in assisting the m^{th} node's transmissions is $a_{mu} \sum_{n \in \mathcal{N}_m^l} \hat{p}_{u,n}^{l}$.

In the presence of the two classes of traffic, service differentiation is indispensable for effective QoS provisioning, where RG nodes are assigned higher priority over BE nodes. As a consequence, node cooperation should also be prioritized. In particular, we consider that only RG nodes can receive assistance from either BE nodes or other RG nodes. Here, we further divide our Phase-3 resource allocation into two steps, namely 1) BE-assisting-RG and 2) RG-assisting-RG.

Step 1: In the case of BE-assisting-RG, allow BE nodes to assist RG nodes whenever favorable. Let $\mathcal{A} = \left\{ m \mid m \in \mathcal{M}_1, \sum_{j \neq m} z_{mj} = 0 \right\}$ and $\mathcal{B} = \left\{ u \mid u \in \mathcal{M}_2, \sum_{i \neq u} z_{iu} = 0 \right\}$. Set $\mathcal{A}$ consists of RG nodes which do not receive any assistance from any other nodes, whereas set $\mathcal{B}$ consists of BE nodes which do not offer any assistance to any nodes. The partner allocation criterion is as follows. For the u^{th} node, $u \in \mathcal{B}$, choose m^* such that $m^* = \arg\max_{m \in \mathcal{A}} \left\{ \frac{U_m'(R_m(\mathbf{a},\mathbf{z})|\mathbf{\Theta})}{a_{mu}} \frac{\partial R_m(\mathbf{a},\mathbf{z})}{\partial z_{mu}} \right\}$.

$$R_{m^*}(\mathbf{a},\mathbf{z}) = \sum_{n=1}^{N}\sum_{l=1}^{L} c^l_{m^*,n}\log_2\left(1+g^l_{m^*m^*,n}p^l_{m^*,n}\right) \tag{22}$$

$$R_{m^*}(\tilde{\mathbf{a}},\tilde{\mathbf{z}}) = \sum_{n=1}^{N}\sum_{l=1}^{L} \frac{1}{2}c^l_{m^*,n}\log_2\left(\left(1+g^l_{m^*m^*,n}p^l_{m^*,n}\right)^2 + a_{m^*u}g^l_{m^*u,n}\hat{p}^l_{u,n}\right) > R_{m^*}(\mathbf{a},\mathbf{z}) \tag{23}$$

$$R_u(\mathbf{a},\mathbf{z}) = \sum_{n=1}^{N}\sum_{l=1}^{L} c^l_{u,n}\log_2\left(1+g^l_{uu,n}p^l_{u,n}\right) \tag{24}$$

$$R_u(\tilde{\mathbf{a}},\tilde{\mathbf{z}}) = \sum_{n=1}^{N}\sum_{l=1}^{L} c^l_{u,n}\log_2\left(1+a_{uu}g^l_{uu,n}p^l_{u,n}\right) < R_u(\mathbf{a},\mathbf{z}) \tag{25}$$

Then, check if this partner allocation process can help enhance the total utilities. Let $R_m(\mathbf{a},\mathbf{z})$ and $R_m(\tilde{\mathbf{a}},\tilde{\mathbf{z}})$ be the achievable data rate obtained of the m^{th} node without node cooperation and that with node cooperation, respectively. We have (22)-(25) shown at the top of this page. Since $R^d_u = 0, \forall u \in \mathcal{M}_2$, the solutions obtained by considering node cooperation are also feasible to the NCRAOP. Set $z_{m^*u} = 1$ and remove the m^{*th} node from $\mathcal{A}$ (i.e., $\mathcal{A} \leftarrow \mathcal{A} - \{m^*\}$) if the following condition is valid:

$$\begin{aligned} &U_{m^*}\left(R_{m^*}(\tilde{\mathbf{a}},\tilde{\mathbf{z}})|\mathbf{\Theta}\right) + U_u\left(R_u(\tilde{\mathbf{a}},\tilde{\mathbf{z}})|\mathbf{\Theta}\right) \\ &> U_{m^*}\left(R_{m^*}(\mathbf{a},\mathbf{z})|\mathbf{\Theta}\right) + U_u\left(R_u(\mathbf{a},\mathbf{z})|\mathbf{\Theta}\right). \end{aligned} \tag{26}$$

If (26) is satisfied, it means that assigning the u^{th} node to the m^{*th} node as its partner can increase the total utilities, thereby improving the network-wise system performance. The u^{th} node is removed from $\mathcal{B}$ (i.e., $\mathcal{B} \leftarrow \mathcal{B} - \{u\}$), and the process repeats until $\mathcal{A} = \{\phi\}$ or $\mathcal{B} = \{\phi\}$.

Step 2: In the case of RG-assisting-RG, allow an RG node to assist other RG nodes whenever favorable. Partner allocation in this step becomes convoluted, for an RG node decreases its achievable data rate and plausibly voids its own rate constraint (given in (6)) when assisting other nodes. Let $\mathcal{C} = \left\{m \mid m \in \mathcal{M}_1, \sum_{j\neq m} z_{mj} = 0\right\}$ and $\mathcal{D} = \left\{j \mid j \in \mathcal{M}_1, \sum_{i\neq j} z_{ij} = 0\right\}$. Set $\mathcal{C}$ consists of the RG nodes which do not receive any assistance from any other nodes, whereas set $\mathcal{D}$ consists of the RG nodes which do not offer any assistance to any RG nodes. For $j \in \mathcal{D}$, choose m^* such that $m^* = \arg\max_{m\in\mathcal{C}\setminus\{j\}}\left\{\frac{U'_m(R_m(\mathbf{a},\mathbf{z})|\mathbf{\Theta})}{a_{mj}}\frac{\partial R_m(\mathbf{a},\mathbf{z})}{\partial z_{mj}}\right\}$. Then, check if the new resource allocation solutions are still feasible for the NCRAOP and can increase the total utilities. Let $(\mathbf{a},\mathbf{z})$ and $(\tilde{\mathbf{a}},\tilde{\mathbf{z}})$ denote the current node cooperative resource allocation solution and the new node cooperative resource allocation solution, respectively. We have (27)-(30) shown on the next page. Set $z_{m^*j} = 1$ and remove the m^{*th} node from $\mathcal{C}$ (i.e., $\mathcal{C} \leftarrow \mathcal{C} - \{m^*\}$) if the following two conditions are valid:

$$\begin{aligned} &U_{m^*}\left(R_{m^*}(\tilde{\mathbf{a}},\tilde{\mathbf{z}})|\mathbf{\Theta}\right) + U_j\left(R_j(\tilde{\mathbf{a}},\tilde{\mathbf{z}})|\mathbf{\Theta}\right) \\ &> U_{m^*}\left(R_{m^*}(\mathbf{a},\mathbf{z})|\mathbf{\Theta}\right) + U_j\left(R_j(\mathbf{a},\mathbf{z})|\mathbf{\Theta}\right) \end{aligned} \tag{31}$$

$$R_j(\tilde{\mathbf{a}},\tilde{\mathbf{z}}) \geq R^d_j. \tag{32}$$

Since $R^d_j > 0, \forall j \in \mathcal{M}_1$, we have to ensure that the rate constraints for all the RG nodes are not violated due to the aforesaid partner allocation (i.e., condition (32)). Condition (31) refers to the case where allocating the j^{th} node as a partner to the m^{*th} node can increase the total utilities. The j^{th} node is removed from $\mathcal{D}$ (i.e., $\mathcal{D} \leftarrow \mathcal{D} - \{j\}$), and the process repeats until $\mathcal{C} = \{\phi\}$ or $\mathcal{D} = \{\phi\}$.

With effective node cooperation, Phase-3 resource allocation improves the Phase-2 resource allocation solutions, thereby giving rise to higher total utilities.

Phase-4: The introduction of partner allocation (i.e., $(\mathbf{a},\mathbf{z})$) in Phase 3 changes the achievable rate function. Thus, the power allocation solution obtained in Phase 2 is no longer optimal. With the known solutions for subcarrier allocation and partner allocation, carry out water filling for power allocation again so as to further improve the system performance. Suppose the u^{th} node is to assist the m^{th} node, i.e., $z_{mu} = 1$. For the sake of optimality, water filling for the u^{th} node should be performed over both $\mathcal{N}^l_u$ and $\mathcal{N}^l_m$; however, procuring the optimal power allocation solutions requires a considerable number of recursive computations. Here, to balance the computational complexity and the system performance, we make use of water filling for power allocation for the m^{th} node over $\mathcal{N}^l_m$ only, $\forall m, l$.

Lemma 1: With the subcarrier allocation solution and the partner allocation solution, denoted by $\tilde{\mathbf{c}}$ and $(\tilde{\mathbf{a}},\tilde{\mathbf{z}})$, respectively, the power allocation solution obtained from water filling, denoted by $\mathbf{p}^*$, is given by

$$p^{*l}{}_{m,n} = \tilde{c}^l_{m,n}\left[\frac{-\left(2{\xi^{(2)}}^l{}_m - \Upsilon\tilde{a}^l_{mm}g^l_{mm,n}\right)}{2{\xi^{(2)}}^l{}_m\tilde{a}^l_{mm}g^l_{mm,n}} + \frac{\sqrt{\Upsilon^2(\tilde{a}^l_{mm})^2(g^l_{mm,n})^2 - 4({\xi^{(2)}}^l{}_m)^2\Gamma_m}}{2{\xi^{(2)}}^l{}_m\tilde{a}^l_{mm}g^l_{mm,n}}\right]^+, \ \forall m,n,l \tag{33}$$

$$R_{m^*}(\mathbf{a},\mathbf{z}) = \sum_{n=1}^{N}\sum_{l=1}^{L} c_{m^*,n}^{l} \log_2\left(1 + a_{m^*m^*} g_{m^*m^*,n}^{l} p_{m^*,n}^{l}\right) \tag{27}$$

$$R_{m^*}(\tilde{\mathbf{a}},\tilde{\mathbf{z}}) = \sum_{n=1}^{N}\sum_{l=1}^{L} \frac{1}{2} c_{m^*,n}^{l} \log_2\left(\left(1 + a_{m^*m^*} g_{m^*m^*,n}^{l} p_{m^*,n}^{l}\right)^2 + a_{m^*j} g_{m^*j,n}^{l} \hat{p}_{j,n}^{l}\right) > R_{m^*}(\mathbf{a},\mathbf{z}) \tag{28}$$

$$R_{j}(\mathbf{a},\mathbf{z}) = \sum_{n=1}^{N}\sum_{l=1}^{L} \frac{1}{2} c_{j,n}^{l} \log_2\left(\left(1 + g_{jj,n}^{l} p_{j,n}^{l}\right)^2 + \sum_{i\neq j} z_{ji} a_{ji} g_{ji,n}^{l} \hat{p}_{i,n}^{l}\right) \tag{29}$$

$$R_{j}(\tilde{\mathbf{a}},\tilde{\mathbf{z}}) = \sum_{n=1}^{N}\sum_{l=1}^{L} \frac{1}{2} c_{j,n}^{l} \log_2\left(\left(1 + a_{jj} g_{jj,n}^{l} p_{j,n}^{l}\right)^2 + \sum_{i\neq j} z_{ji} a_{ji} g_{ji,n}^{l} \hat{p}_{i,n}^{l}\right) < R_{j}(\mathbf{a},\mathbf{z}) \tag{30}$$

where $\Upsilon = U'_m(R_m(\mathbf{p})|\mathbf{\Theta}) + {\xi^{(1)}}_m$, $\Gamma_m = \sum_{u\neq m} \tilde{z}_{mu}\tilde{a}_{mu} g_{mu,n}^{l} \hat{p}_{u,n}^{l}$, and ${\xi^{(2)}}_m^{l}$ is the Lagrange multiplier for the constraint $\sum_{n=1}^{N} p_{m,n}^{l} \leq P_m^{\max}, \forall m, l$.

Proof: We omit the proof as it is similar to the one given in [22]. ∎

With the aforementioned optimal power allocation, Phase-4 resource allocation further enhances the Phase-3 resource allocation solution, leading to higher total utilities.

The flowchart of our proposed centralized approach is depicted in Fig. 2.

D. Proposed Approach with Distributed Control

When clusterheads are not available, distributed node cooperative resource allocation is essential. We consider that each mesh node can communicate with all other mesh nodes in the same cluster. Here, we propose a two-phase distributed node cooperative resource allocation approach with QoS support and service differentiation. We consider that an active resource allocation interval consists of two phases, namely contention phase and transmission phase. In the contention phase, the approach of Black-burst can be used for subcarrier contention [2]. In the transmission phase, mesh nodes transmit their data with the consideration of node cooperation, if feasible and favorable.

1) Contention Phase: A contention phase consists of a number of contention periods. For each contention period, the Black-burst (BB) methodology is used for the subcarrier contention to achieve service differentiation [2]. Let $\mathcal{E} = \left\{m \mid m \in \mathcal{M}_1, R_m(\cdot) < R_m^d\right\}$ and $\mathcal{F} = \left\{m \mid m \in \mathcal{M}_1, R_m(\cdot) \geq R_m^d\right\} \bigcup \{m \mid m \in \mathcal{M}_2\}$. Set $\mathcal{E}$ consists of the RG nodes whose QoS demands are not satisfied, whereas set $\mathcal{F}$ consists of both the BE nodes and the RG nodes whose QoS demands are met. Each contention period is further divided into two mini-periods, where the first mini-period is for the contention among the nodes in $\mathcal{E}$, while the second mini-period is for the contention among the nodes in $\mathcal{F}$. Fig. 3(a) depicts the dynamics of a contention phase.

At the beginning of each contention period, every node is in a listening mode and waits for a period of time before transmitting its BB signal. In the first mini-period, the waiting time of an RG node in $\mathcal{E}$ is inversely proportional to its minimum required rate. Therefore, the node with the highest minimum required rate sends its BB signal earlier than the other RG nodes in $\mathcal{E}$ so as to win the contention. Other nodes which detect the BB signal remain in the listening mode. An RG node becomes a winner for this contention if it senses an idle channel after transmitting a BB signal. To ensure that each contention period results in only one winner, we assume that the length of a BB signal sent from a node is proportional to its network ID (e.g., MAC address). The winner of this contention period then selects the best subcarriers according to the subcarrier allocation criterion given in (10) so as to meet its QoS demand. Notice that uniform power allocation is employed when the subcarriers are selected. After the subcarrier selection is finished, the winner transmits a BB signal over the allocated subcarriers so that the other nodes in a listening mode can detect and record which subcarriers have been chosen. Then, all the other RG nodes wait for the next contention and this process repeats until all the RG nodes in $\mathcal{E}$ have selected their subcarriers. Since we assume that CAC is in place, all the QoS requirements of the RG nodes in $\mathcal{E}$ can be met at the end of this phase.

Subcarrier contention among the nodes in $\mathcal{F}$ (i.e., satisfied RG nodes and BE nodes) occurs only if there is some unallocated subcarrier(s). If there is no BB detected in the first mini-period, meaning that the subcarrier contention among the RG nodes in $\mathcal{E}$ is complete, every node in $\mathcal{F}$ waits for a period of time in the second mini-period before sending out its BB signal, where the waiting time is inversely proportional to its marginal utility increase when choosing the best available subcarrier (i.e., $\frac{\partial U_m(R_m(\cdot))}{\partial c_{m,n}^{l}}$). Thus, the larger the marginal utility increases, the more likely that the node will be the winner. The winner then selects the best subcarrier according to the subcarrier allocation criterion given in (10). The process repeats until all the subcarriers are used. Similar to the centralized resource allocation approach, after the subcarrier allocation is determined, each mesh node performs water filling for power allocation independently to further increase both its utility and the system performance.

2) Transmission Phase: A transmission phase consists of a number of frames, where each frame consists of L DATA slots. Each DATA slot is further divided into two (identical) minislots. Fig. 3(b) depicts the frame structure used for a transmission phase. Fig. 4 illustrates a typical (non-altruistic)

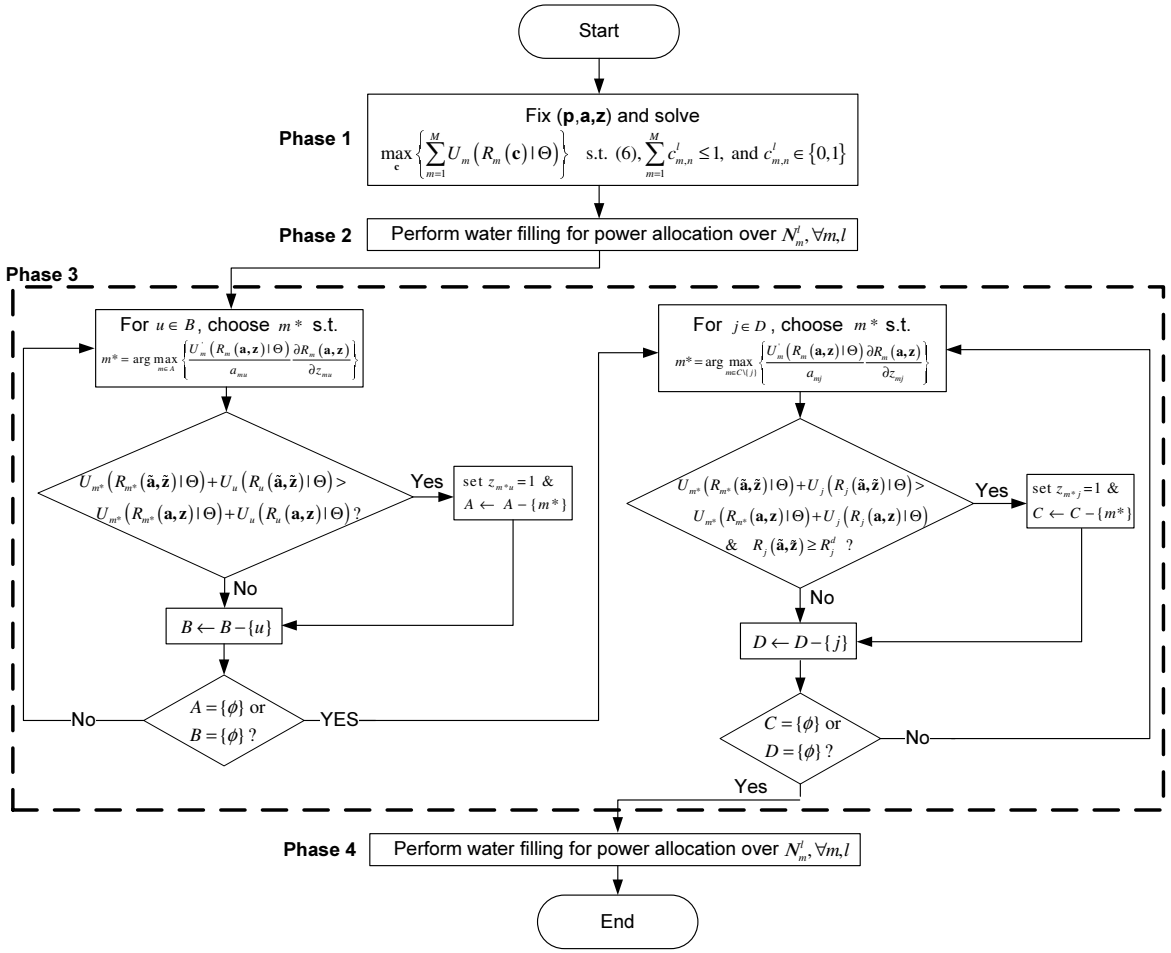

Fig. 2. Flowchart of the proposed centralized approach.

node cooperation scenario in the transmission phase. In Fig. 4(a), the m^{th} node (i.e., an RG node) is transmitting data to its destination node (i.e., the d^{th} node) in the first minislot. The m^{th} node's transmission can be overheard by the u^{th} node in the first minislot if the u^{th} node is in the listening mode. The u^{th} node then checks if it can decode the m^{th} node's transmissions successfully. If the u^{th} node fails to decode the m^{th} node's transmissions, the u^{th} node will not help relay the m^{th} node's data (see Fig. 4(b)). On the other hand, if the u^{th} node can decode the m^{th} node's transmissions reliably, the u^{th} node then becomes the partner of the m^{th} node if condition (26) is valid with the u^{th} node being a BE node or conditions (31) and (32) are valid with the u^{th} node being an RG node (see Fig. 4(c)). As a matter of fact, the m^{th} node can have more than one partner at a time (e.g., the i^{th} node and u^{th} node in Fig. 4(c)). In the presence of multiple potential partners, we employ the partner selection scheme proposed in [12] to choose the best partner for the m^{th} node with respect to our partner selection criterion given in (12). We also assume that a signal capture mechanism is in place so that a potential partner can only overhear the strongest neighboring node's transmission [23]. This node cooperation between a source node and its partner sustains until the next active interval.

E. Complexity Analysis

The time complexity of the proposed four-phase centralized approach is $O(bMNL + |\mathcal{M}_1|M)$, where b is a constant. For the proposed two-phase distributed approach, since each mesh node behaves independently, the time complexity is $O(kNL + M)$, where k is a constant. It is noteworthy that the difference in time complexity between the two approaches stems from different modes of network operation (i.e., centralized control or distributed control) and different methodologies of resource allocation (i.e., partner allocation or partner selection). For comparison, the time complexity of a Hungarian approach is $O(|\mathcal{M}_1|M^2 + MN^2L^2)$. Despite a plausibly improved system performance, applying a Hungarian approach can be inefficient in the WMNs without powerful centralized controllers. In contrast, our proposed approaches are of low complexity and more suitable for the low-cost mesh nodes.

F. Discussion

In game theory, efficient resource utilization is determined by the concept of *Pareto optimality* [24]. On the other hand, network stability can be achieved when a resource allocation solution attains an *Nash equilibrium* [24]. Following the definitions of Pareto optimality and Nash equilibrium, we can show that the partner allocation/selection solutions in our proposed node cooperative resource allocation approaches

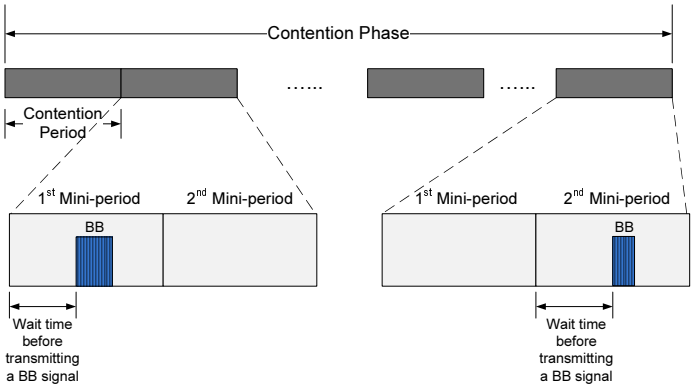

(a) An illustration of the subcarrier contention phase among RG nodes and BE nodes.

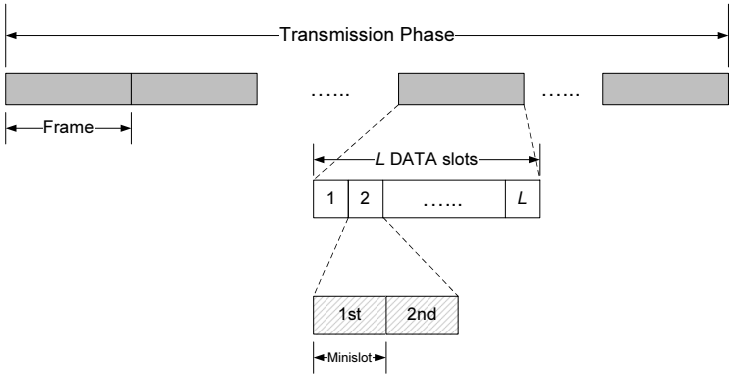

(b) The structures of a frame and a DATA slot employed in the transmission phase.

Fig. 3. The phase structures of the proposed two-phase distributed node cooperative resource allocation approach.

are Pareto optimal. Further, modeled by a round-robin game played by the RG nodes (potential partners), the partner selection (allocation) solutions attain an Nash equilibrium. The proof for our proposed partner allocation achieving Pareto optimality is reported in [1]. Other game-theoretic evaluation results can be proved directly by first principles. Therefore, our proposed approaches not only can make efficient use of scarce network resources but also can facilitate network stability.

The flowchart of our proposed distributed approach is depicted in Fig. 5.

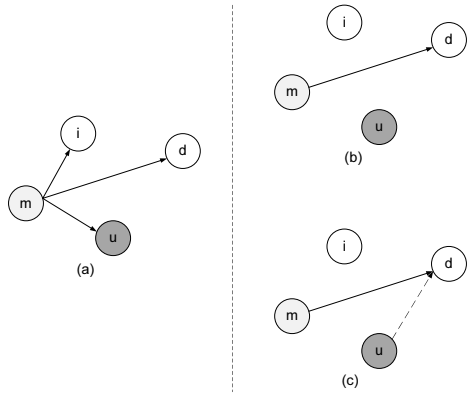

Fig. 4. Example of a typical node cooperation scenario in the transmission phase.

VI. Performance Evaluation

A. Packet-Level QoS Provisioning

In the MAC layer, to streamline QoS provisioning and provide service differentiation, packet prioritization is imperative [25]. We conceive that the priority of RG traffic (packets) is related to the performance of their packet dropping rates. In this work, we only take the packet dropping due to the delay bound violation into account. The higher the packet dropping rate that an RG traffic flow suffers from, the higher the priority of the packets associated with that flow. In the centralized approach, after gathering the transmission requests in the control slot, a clusterhead grants the requests of transmitting higher-priority packets first. In the distributed approach, we consider that the RG node with the highest packet dropping rate transmits its BB signal earlier than the other nodes in the contention phase. If two or more RG nodes have the same packet dropping rate, the node with the highest minimum required rate will win the contention of interest. In

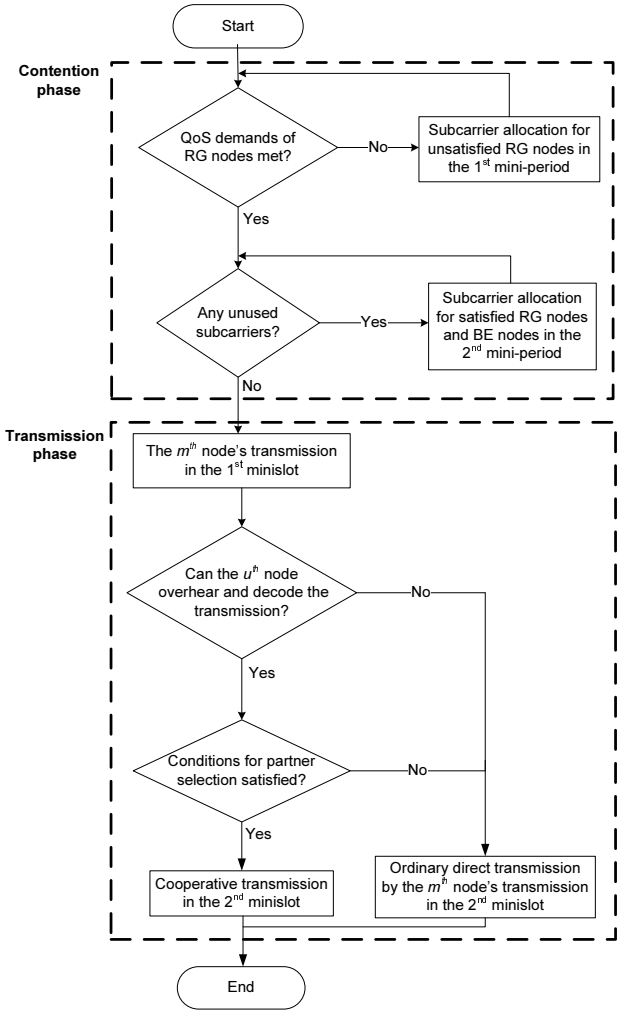

Fig. 5. Flowchart of the proposed distributed approach.

other words, our QoS provisioning strategy for the RG traffic hinges upon the packet dropping rate. To further augment the effectiveness of QoS provisioning, the partners, timeslots, and subcarriers allocated to or chosen by a particular mesh node are reserved for packet transmissions until the next active resource allocation interval (e.g., next polling).

B. Simulation Environment

Consider a cluster with a number of wireless mesh nodes randomly located in a 1km x 1km coverage area. We adopt the path-loss model suggested in [26] (i.e., hilly/moderate-to-heavy tree density). Consider an OFDM-based wireless environment with N available subcarriers. We assume that all subcarriers exhibit frequency-flat Rayleigh fading. The maximum transmission rate over each subcarrier is considered to be 200kb/s. We further assume that the routing is predetermined so that the transmission source and destination pair of an incoming packet is known in advance. Other simulation parameters are chosen as follows: $P_m^{\max} = 1$W, $\sigma_n^2 = 10^{-12}$W, $N = 100$, $L = 4$, $\rho = 1/3$, $\varphi = 1$, and $\mathbf{\Theta} = 1$. Since our resource allocation solutions sustain for an active resource allocation interval, the duration of the first frame (with 1 beacon slot, 1 control slot and L DATA slots) is $5(L + 2)$ ms and that of the subsequent frames (with L DATA slots) is $5L$ ms in the proposed centralized approach, with a 5ms DATA slot. We consider that the polling is done in every T ms, meaning that the node cooperative resource allocation solution is updated every T ms. Here, both the polling and the beacon packet transmissions are assumed to be error-free. For fair comparison, we consider that the duration of an active interval in the proposed distributed approach is T ms, where the first 10ms is dedicated to the contention phase while the remaining time period is dedicated to the transmission phase. We perform the simulations for 10,000 runs and average the results, where each simulation run sustains 5,000 frames.

Concerning the traffic models, the RG traffic is generated according to a two-state ON-OFF model. In the ON state, a fixed-size packet arrives in every 20ms with rate demand 384kb/s, whereas in the OFF state, no packet is generated. We consider that the duration of an ON period and that of an OFF period are independent, both follow an exponential distribution, where the mean ON period and the mean OFF period are 1s and 1.2s, respectively. The delay bound of RG traffic is assumed to be $5L$ ms. The required packet dropping rate is less than 1%. On the other hand, the BE traffic does not have any QoS requirements. BE packet arrivals follow a Poisson process with mean rate λ packets/second, where the packet size follows a Weibull distribution (i.e., Weibull(2,2)). To mimic the mixed traffic in a WMN, we assume that an RG node has one RG traffic flow and one BE flow, while a BE node has one BE flow.

C. Simulation Results

We evaluate the system performance of the proposed node cooperative resource allocation approaches versus M, T, $|\mathcal{M}_1|$, and λ in terms of throughput, resource utilization, packet dropping rate, and node cooperation gain (i.e., normalized throughput gain due to node cooperation). The standard deviations of the results are also plotted for reference. For performance comparison, we consider two baseline approaches and an approach suggested in [17]: 1) a centralized baseline approach which is the same as the proposed centralized approach without Phase-3 and Phase-4 resource allocation; 2) a distributed baseline approach which is the same as the proposed distributed approach without considering node cooperation in the transmission phase; and 3) the Zhang's approach proposed in [17] which first allocates the subcarriers with no QoS consideration to maximize throughput and then re-allocates the subcarriers trying to satisfy the QoS demands of the nodes without considering node cooperation. Note that the performance degradation due to signalling overhead is not taken into account in evaluating the system performance. An upper bound[1] for average throughput performance is also plotted for reference.

1) Effect of M: For $|\mathcal{M}_2| = 2|\mathcal{M}_1|$, $T = 150$ms, and $\lambda = 50$ packets/second, Fig. 6 shows the throughput performance versus the number of mesh nodes. We can see that the throughputs of all considered approaches increase with

[1]We analytically obtain an upper bound for average throughput performance under the assumptions of no packet dropping for the RG traffic and perfect statistical traffic multiplexing.

TABLE II
RELATIONSHIP BETWEEN THE NUMBER OF MESH NODES, M, AND THE NODE COOPERATION GAIN (NCG) (I.E., NORMALIZED THROUGHPUT GAIN DUE TO NODE COOPERATION) FOR THE PROPOSED APPROACHES (WITH $|\mathcal{M}_2| = 2|\mathcal{M}_1|$, $T = 150$MS, AND $\lambda = 50$ PACKETS/SECOND)

M	6	12	18	24	30	36	42	48
NCG for the proposed centralized approach (in %)	4.29	10.11	16.92	21.81	23.14	23.74	23.44	24.21
NCG for the proposed distributed approach (in %)	7.47	7.48	7.50	7.54	7.59	7.89	8.36	9.35

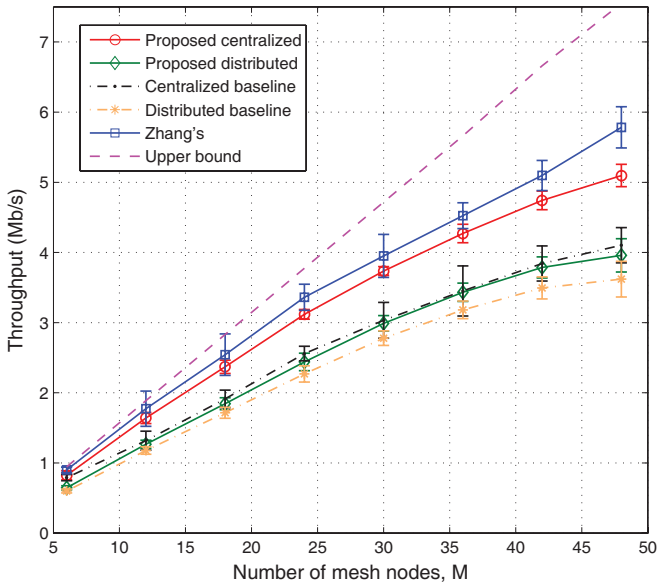

Fig. 6. Comparison of the throughput performance of the proposed four-phase centralized approach, the proposed two-phase distributed approach, the centralized baseline approach, the distributed baseline approach, and the Zhang's approach [17] vs. the number of mesh nodes (with $|\mathcal{M}_2| = 2|\mathcal{M}_1|$, $T = 150$ms, and $\lambda = 50$ packets/second).

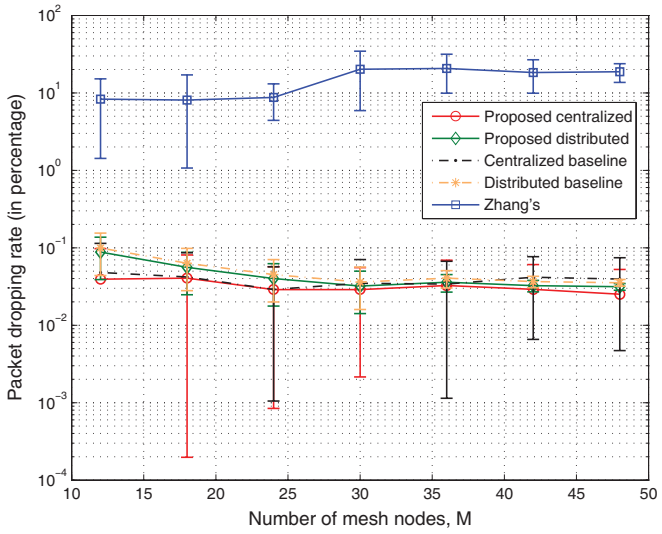

Fig. 7. Comparison of the RG packet dropping rates of the proposed four-phase centralized approach, the proposed two-phase distributed approach, the centralized baseline approach, the distributed baseline approach, and the Zhang's approach [17] vs. the number of mesh nodes (with $|\mathcal{M}_2| = 2|\mathcal{M}_1|$, $T = 150$ms, and $\lambda = 50$ packets/second).

M, since the system is not saturated. As expected, the centralized approaches (i.e., the proposed four-phase centralized approach and the centralized baseline approach) outperform their distributed counterparts (i.e., the proposed two-phase distributed approach and the distributed baseline approach) due to the merit of the existence of a clusterhead. However, the Zhang's approach achieves the highest throughput among all considered approaches, realizing the goal of throughput maximization. On a different note, our proposed four-phase centralized (two-phase distributed) approach outperforms the baseline centralized (distributed) approach, which stems from an additional performance gain due to beneficial node cooperation. The node cooperation gain (NCG) is given in Table II. As anticipated, the more the mesh nodes, the more the potential helpers and hence the higher the NCGs. In general, the NCG obtained in our proposed centralized approach is higher than that obtained in our proposed distributed approach. The rationale is mainly due to the partner *allocation* employed in our proposed centralized approach yet the partner *selection* in our proposed distributed approach. Another reason is that node cooperation in the proposed distributed approach can only be triggered when some mesh nodes are idle in the first minislot, thereby curbing some potential and favorable node cooperation opportunities. The gain in our proposed centralized approach is roughly leveled off from $M = 30$ onward, which is ascribed to the limited available resources (i.e., subcarriers). We expect that the NCG can be higher with a larger value of N. We observe that, as the number of mesh nodes increases from 6 to 48, the resource utilization of the proposed four-phase centralized approach increases from 9% to 41%, that of the proposed two-phase distributed approach from 7% to 30%, that of the centralized baseline approach from 8% to 31%, that of the distributed baseline approach from 6% to 28%, and that of the Zhang's approach from 10% to 44%, respectively. The low resource utilization is due to low traffic load and resource reservation. We observe that the resource utilization (and throughput) for our proposed approaches can be improved when the traffic load increases and the RG traffic demand is less stringent. In Fig. 7, the RG packet dropping rates are depicted. The packet dropping rates for RG traffic in our proposed approaches and two baseline approaches are well below 1% due to effective packet-level QoS provisioning. On the other hand, the RG packet dropping rate of the Zhang's approach increases and reaches 20% as M increases. Fig. 7 shows that the Zhang's approach is ineffective in supporting the QoS requirements of RG traffic at the packet level. Nonetheless, the Zhang's approach aims at maximizing the (network-wise) throughput in lieu of focusing on (node-wise) QoS satisfaction. The results also assure the fact that provisioning QoS and increasing throughput are conflicting performance measures [19].

TABLE III
RELATIONSHIP BETWEEN THE VALUE OF T AND THE NODE COOPERATION GAIN (NCG) (I.E., NORMALIZED THROUGHPUT GAIN DUE TO NODE COOPERATION) FOR THE PROPOSED APPROACHES (WITH $M = 30$ MESH NODES, $|\mathcal{M}_2| = 2|\mathcal{M}_1|$, AND $\lambda = 50$ PACKETS/SECOND)

T (in ms)	20	50	150	300	1000
NCG for the proposed centralized approach (in %)	21.13	22.46	23.15	32.50	54.05
NCG for the proposed distributed approach (in %)	5.48	6.99	7.58	11.06	13.71

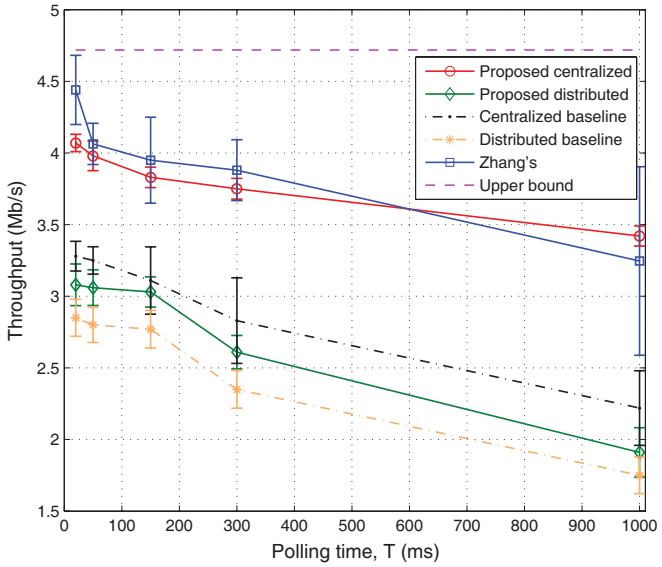

Fig. 8. Comparison of the throughput performance of the proposed four-phase centralized approach, the proposed two-phase distributed approach, the centralized baseline approach, the distributed baseline approach, and the Zhang's approach [17] vs. the polling time (with $M = 30$ mesh nodes, $|\mathcal{M}_2| = 2|\mathcal{M}_1|$, and $\lambda = 50$ packets/second).

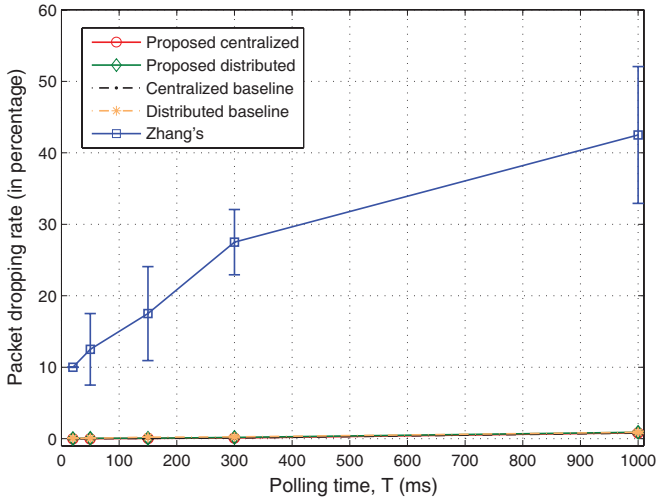

Fig. 9. Comparison of the RG packet dropping rates of the proposed four-phase centralized approach, the proposed two-phase distributed approach, the centralized baseline approach, the distributed baseline approach, and the Zhang's approach [17] vs. the polling time (with $M = 30$ mesh nodes, $|\mathcal{M}_2| = 2|\mathcal{M}_1|$, and $\lambda = 50$ packets/second).

2) Effect of T: For $M = 30$ mesh nodes, $|\mathcal{M}_2| = 2|\mathcal{M}_1|$, and $\lambda = 50$ packets/second, we study the impact of the polling time (or the length of an active interval) on the system performance measures. Fig. 8 shows the throughput performance versus the value of T. The throughputs obtained in all considered approaches decrease with the value of T. The larger the value of T, the less accurate the traffic load estimate and hence the weaker the throughput performance. In particular, even though our proposed distributed approach maintains its NCG against T (see Table III), its throughput drops significantly from 3.0Mb/s to 1.9Mb/s. On the contrary, with the help of a clusterhead, not only does our proposed centralized approach effectively sustain its throughput performance, but its NCG also ramps up considerably from 21% to 54% when T increases (see Table III). As a result, the proposed four-phase centralized approach is shown to be less vulnerable to poor traffic load estimates. As to the Zhang's approach, however, its throughput obtained plummets sharply as T increases. The decline is due to the absence of effective packet-level QoS provisioning mechanism in place and, therefore, once the traffic load estimates are less accurate, the system performance deteriorates dramatically. This phenomenon can also be explained in Fig. 9. Similar to Fig. 7, the RG packet dropping rates of our proposed approaches and two baseline approaches are capped by 1%. In contrast, the packet dropping rate of the Zhang's approach increases from 10% to 43%, resulting in the worst RG packet dropping rate performance. In short, resource allocation approaches without considering packet-level QoS provisioning are susceptible to the accuracy of traffic load estimates. For resource utilization, we observe that the trends of all curves are similar to those in Fig. 8.

3) Effect of $|\mathcal{M}_1|$: For $M = 30$ mesh nodes, $T = 150$ms, and $\lambda = 50$ packets/second, we study the impact of RG traffic (i.e., the value of $|\mathcal{M}_1|$) on the system performance measures. In Fig. 10, the throughput performance versus the value of $|\mathcal{M}_1|$ is depicted. Since the network is not saturated, in general, all the curves go up with the number of RG nodes, $|\mathcal{M}_1|$. From $|\mathcal{M}_1| = 20$ onward, the throughputs of our proposed distributed approach and the distributed baseline approach begin to level off, resulting from the effect of resource reservation for the RG traffic. By the same token, the rates of the throughput increment in our proposed centralized approach and the centralized baseline approach decrease from $|\mathcal{M}_1| = 25$ onward. The throughput performance of the Zhang's approach first rises from $|\mathcal{M}_1| = 10$ to 20 and then declines afterwards. Similar to the previous discussions, as the number of RG nodes increases, the Zhang's approach fails to effectively provision packet-level QoS, thereby increasing its RG packet dropping rate and decreasing its throughput. At $|\mathcal{M}_1| = 30$, the throughput obtained in the Zhang's approach is even lower than that in the proposed four-phase centralized approach. The resource utilizations attained by all the approaches have the trends similar to those in Fig. 10.

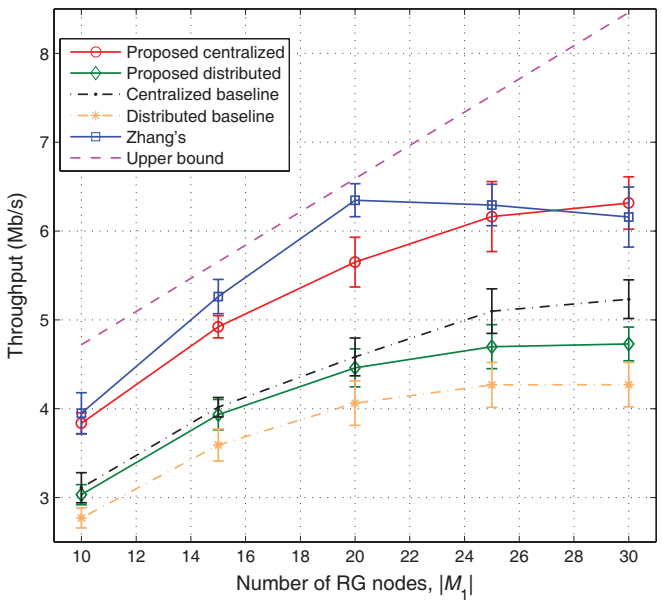

Fig. 10. Comparison of the throughput performance of the proposed four-phase centralized approach, the proposed two-phase distributed approach, the centralized baseline approach, the distributed baseline approach, and the Zhang's approach [17] vs. the number of RG nodes (with $M = 30$ mesh nodes, $T = 150$ms, and $\lambda = 50$ packets/second).

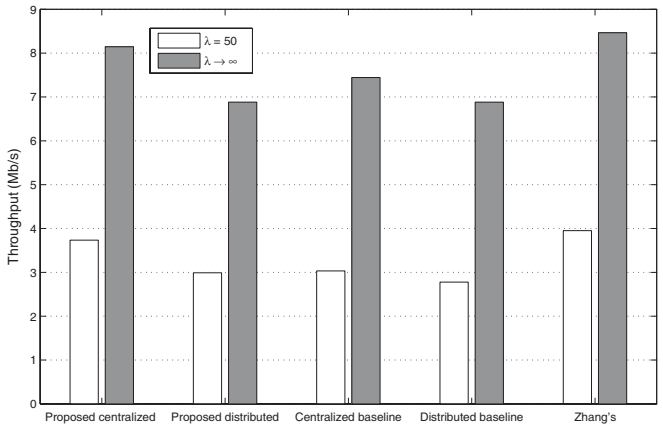

Fig. 11. Comparison of the throughput performance of the proposed four-phase centralized approach, the proposed two-phase distributed approach, the centralized baseline approach, the distributed baseline approach, and the Zhang's approach [17] vs. the value of λ (with $M = 30$ mesh nodes, $|\mathcal{M}_2| = 2|\mathcal{M}_1|$, and $T = 150$ms).

We observe that the NCGs of our two proposed approaches stay more or less the same against $|\mathcal{M}_1|$. It shows that the node cooperation opportunities of both proposed approaches are almost independent of the number of RG nodes in the system. It is noteworthy that, in Fig. 10, there is an obvious performance gap between the throughputs obtained from the considered approaches and the upper bound at a large $|\mathcal{M}_1|$. This gap is mainly ascribed to the resource reservation for RG traffic. Concerning the RG packet dropping rates, the trends of the considered approaches are similar to the ones shown in Fig. 9. In a nutshell, with the virtue of node cooperation, our four-phase centralized approach can achieve better system performance and provide more effective QoS provisioning than its throughput-oriented counterpart when there is a large number of RG nodes in the network.

4) Effect of λ: For $M = 30$ mesh nodes, $|\mathcal{M}_2| = 2|\mathcal{M}_1|$, $T = 150$ms, and $\rho = 1/3$, we study the impact of BE traffic (i.e., the value of λ) on the system performance measures. Here, we consider two cases: 1) $\lambda = 50$ packets/second (i.e., bursty data traffic) and 2) $\lambda \to \infty$ packets/second (i.e., background data traffic). Fig. 11 shows the throughput performance for $\lambda = 50$ and $\lambda \to \infty$. It is clear that the throughputs in the presence of background data traffic (i.e., $\lambda \to \infty$) are higher than in the case of Poisson arrivals (i.e., $\lambda = 50$). We also observe that the NCGs obtained drop from 23.14% to 9.01% in the proposed centralized approach and from 7.59% to 0% in the proposed distributed approach, respectively, when the data traffic changes from bursty (i.e., $\lambda = 50$) to background (i.e., $\lambda \to \infty$). Concerning our proposed centralized approach, since the rate function is a concave function and the throughput obtained by Phase-1 and Phase-2 resource allocation is already high in the case of $\lambda \to \infty$, the room for further throughput increment due to node cooperation is relatively smaller than in the case of $\lambda = 50$. As a result, the performance gain of the proposed four-phase centralized approach over the centralized baseline approach is less substantial. On the other hand, it is notable that the NCG of our proposed distributed approach vanishes in the case of $\lambda \to \infty$, the rationale for which is that all the mesh nodes are busy all the time and no mesh nodes are idle in the first minislot in the transmission phase. Thus, there is no partner available, wiping out the effectiveness of node cooperation. In other words, if a WMN with decentralized control is saturated (with background data traffic), the benefits of non-altruistic node cooperation cannot be exploited. In a nutshell, when designing and deploying an efficient and effective WMN in practice, we should take notice of the nature of node cooperation (i.e., non-altruistic or altruistic), the traffic pattern (i.e., bursty traffic or background traffic), and the mode of network operation (i.e., centralized control or distributed control). As regards the packet dropping rate of the RG traffic, we observe that the results are nearly the same as the ones shown in Fig. 7. All in all, the BE packets are assigned the lower priority and hence the change in the value of λ has almost no influence on the packet dropping rate performance of RG traffic.

VII. Conclusions

In this paper, we propose two non-altruistic node cooperative resource allocation approaches tailored for WMNs with QoS support and service differentiation. Both the proposed four-phase centralized approach and the proposed two-phase distributed approach are shown to be effective in QoS provisioning for RG traffic and system performance improvement. Simulation results demonstrate that our proposed approaches achieve satisfactory system performance as the number of mesh nodes changes and are less susceptible to the inaccuracy of traffic load estimates. Our study reveals a crucial design principle that whether or not node cooperation is useful depends upon the nature of node cooperation, the traffic pattern, and the mode of network operation. Further, our approaches

are of low complexity, leading to a viable candidate for practical implementation.

REFERENCES

[1] H. T. Cheng and W. Zhuang, "QoS-driven node cooperative resource allocation for wireless mesh networks with service differentiation," in *Proc. IEEE GLOBECOM*, 2009, accepted for presentation.

[2] H. T. Cheng, H. Jiang, and W. Zhuang, "Distributed medium access control for wireless mesh networks," *Wireless Commun. and Mobile Computing*, vol. 6, no. 6, pp. 845–864, Sep. 2006.

[3] J. Ishmael, S. Bury, D. Pezaros, and N. Race, "Deploying rural community wireless mesh networks," *IEEE Internet Computing*, vol. 12, no. 4, pp. 22–29, July-Aug. 2008.

[4] H. T. Cheng and W. Zhuang, "Pareto optimal resource management for wireless mesh networks with QoS assurance: joint node clustering and subcarrier allocation," *IEEE Trans. Wireless Commun.*, vol. 8, no. 3, pp. 1573–1583, Mar. 2009.

[5] R. U. Nabar, H. Blcskei, and F. W. Kneubhler, "Fading relay channels: performance limits and spacetime signal design," *IEEE J. Sel. Areas Commun.*, vol. 22, no. 6, pp. 1099–1109, Aug. 2004.

[6] J. N. Laneman, D. N. C. Tse, and G. W. Wornell, "Cooperative diversity in wireless networks: efficient protocols and outage behavior," *IEEE Trans. Inf. Theory*, vol. 50, no. 12, pp. 3062–3080, Dec. 2004.

[7] A. Bletsas, A. Khisti, D. Reed, and A. Lippman, "A simple cooperative diversity method based on network path selection," *IEEE J. Sel. Areas Commun.*, vol. 24, no. 3, pp. 659–672, Mar. 2006.

[8] H. T. Cheng, H. Mheidat, M. Uysal, and T. M. Lok, "Distributed space-time block coding with imperfect channel estimation," in *Proc. IEEE ICC*, vol. 1, May 2005, pp. 583–587.

[9] M. K. Karakayali, G. J. Foschini, and R. A. Valenzuela, "Network coordination for spectrally efficient communications in cellular systems," *IEEE Wireless Commun. Mag.*, vol. 13, no. 4, pp. 56–61, Aug. 2006.

[10] H. T. Cheng and T. M. Lok, "Detection schemes for distributed space-time block coding in time-varying wireless cooperative systems," in *Proc. IEEE Tencon'05*, Nov. 2005, pp. 289–293.

[11] V. Mahinthan, L. Cai, J. W. Mark, and X. Shen, "Partner selection based on optimal power allocation in cooperative-diversity systems," *IEEE Trans. Veh. Technol.*, vol. 57, no. 1, pp. 511–520, Jan. 2008.

[12] H. Shan, W. Zhuang, and Z. Wang, "Distributed cooperative MAC for multi-hop wireless networks," *IEEE Commun. Mag.*, vol. 47, no. 2, pp. 126–133, Feb. 2009.

[13] Z. Zhang, J. Shi, H.-H. Chen, M. Guizani, and P. Qiu, "A cooperation strategy based on nash bargaining solution in cooperative relay networks," *IEEE Trans. Veh. Technol.*, vol. 57, no. 4, pp. 2570–2577, July 2008.

[14] J. Huang, Z. Han, M. Chiang, and H. V. Poor, "Auction-based resource allocation for cooperative communications," *IEEE J. Sel. Areas Commun.*, vol. 26, no. 7, pp. 1226–1237, Sep. 2008.

[15] Q.-Q. Zhang, W.-D. Gao, M.-G. Peng, and W.-B. Wang, "Partner selection strategies in cooperative wireless networks with optimal power distribution," *J. China Universities of Posts and Telecommunications*, vol. 15, no. 3, pp. 47–50,58, 2008.

[16] A. Nosratinia and T. E. Hunter, "Grouping and partner selection in cooperative wireless networks," *IEEE J. Sel. Areas Commun.*, vol. 25, no. 2, pp. 369–378, Feb. 2007.

[17] Y. J. Zhang and K. B. Letaief, "Multiuser adaptive subcarrier-and-bit allocation with adaptive cell selection for OFDM systems," *IEEE Trans. Wireless Commun.*, vol. 3, no. 5, pp. 1566–1575, Sep. 2004.

[18] F. P. Kelly, "Charging and rate control for elastic traffic," *European Trans. Telecommun.*, vol. 8, pp. 33–37, 1997.

[19] H. T. Cheng and W. Zhuang, "An optimization framework for balancing throughput and fairness in wireless networks with QoS support," *IEEE Trans. Wireless Commun.*, vol. 7, no. 2, pp. 584–593, Feb. 2008.

[20] S. Boyd and L. Vandenberghe, *Convex Optimization*. Cambridge University Press, 2004.

[21] H. T. Cheng and W. Zhuang, "Joint power-frequency-time resource allocation in clustered wireless mesh networks," *IEEE Network*, vol. 22, no. 1, pp. 45–51, Jan.-Feb. 2008.

[22] G. Song and Y. Li, "Utility-based resource allocation and scheduling in OFDM-based wireless broadband networks," *IEEE Commun. Mag.*, vol. 43, no. 12, pp. 127–134, Dec. 2005.

[23] K. Whitehouse, A. Woo, F. Jiang, J. Polastre, and D. Culler, "Exploiting the capture effect for collision detection and recovery," *IEEE EmNetS-II*, pp. 45–52, May 2005.

[24] G. Owen, *Game Theory, 3rd Ed.* Academic Press, 2001.

[25] H. T. Cheng and W. Zhuang, "Novel packet-level resource allocation with effective QoS provisioning for wireless mesh networks," *IEEE Trans. Wireless Commun.*, vol. 8, no. 2, pp. 694–700, Feb. 2009.

[26] IEEE 802.16 Broadband Wireless Access Working Group, "Channel models for fixed wireless applications," 2003. [Online]. Available: http://www.ieee802.org/16

Ho Ting Cheng (S'05) received the BEng and MPhil degrees in Information Engineering from The Chinese University of Hong Kong in 2003 and 2005, respectively. He is a research assistant and currently working toward his Ph.D. degree at the Department of Electrical and Computer Engineering, University of Waterloo, Canada. His research interests include distributed resource allocation, quality-of-service provisioning, medium access control, scheduling, call admission control, wireless mesh networking, and communication theory.

Weihua Zhuang (M'93-SM'01-F'08) received the B.Sc. and M.Sc. degrees from Dalian Maritime University, China, and the Ph.D. degree from the University of New Brunswick, Canada, all in electrical engineering. Since October 1993 she has been a faculty member in the Department of Electrical and Computer Engineering, University of Waterloo, where she is currently a professor. Her current research focuses on resource allocation and QoS provisioning in wireless networks She is a co-author of the textbook *Wireless Communications and Networking*, and a co-recipient of a Best Paper Award from IEEE ICC 2007, a Best Student Paper Award from IEEE WCNC 2007, and the Best Paper Awards from QShine 2007 and 2008. She received the Outstanding Performance Award in 2005, 2006, and 2008 from the University of Waterloo for outstanding achievements in teaching, research, and service, and the Premier's Research Excellence Award in 2001 from the Ontario Government for demonstrated excellence of scientific and academic contributions. Dr. Zhuang is the Editor-in-Chief of IEEE TRANSACTIONS ON VEHICULAR TECHNOLOGY, and an Editor of IEEE TRANSACTIONS ON WIRELESS COMMUNICATIONS, EURASIP JOURNAL ON WIRELESS COMMUNICATIONS AND NETWORKING, and INTERNATIONAL JOURNAL OF SENSOR NETWORKS. She is a Fellow of IEEE and an IEEE Communications Society Distinguished Lecturer.